Journal of ELECTRONIC MATERIALS, Vol. 40, No. 7, 2011
DOI: 10.1007/s11664-011-1662-5

Synthesis of *c*-Axis Inclined AlN Films in an Off-Center System for Shear Wave Devices

JUAN XIONG,[1] HAO-SHUANG GU,[1,2] WEN WU,[1] MING-ZHE HU,[1] PENG-FEI DU,[1] and HONG XIE[1]

1.—School of Physics and Electronic Technology, Hubei University, Wuhan 430062, China. 2.—e-mail: guhsh583@yahoo.com.cn

AlN thin films are of continuing interest for excitation of acoustic waves in surface and bulk acoustic wave devices. We report herein on preparation and characterization of *c*-axis inclined AlN films by a new method of rotating the substrate holder plate to different angles in an off-center system. The microstructure of the *c*-axis inclined AlN films was investigated using x-ray diffraction, scanning electron microscopy, and transmission electron microscopy. The analyses showed that polycrystalline AlN films with *c*-axis inclination of up to 12° could be obtained using the off-center system. Solidly mounted resonators based on the deposited *c*-axis inclined and vertical AlN films were successfully realized. The frequency responses showed dual-mode resonance characteristics located at 1.12 GHz and 1.87 GHz, corresponding to shear and longitudinal resonant modes, respectively.

Key words: *c*-axis inclined AlN films, sputtering, shear mode, bulk acoustic wave device

INTRODUCTION

Highly textured, e.g., *c*-axis oriented, AlN or ZnO thin films are critically important for fabrication of high-frequency electro-acoustic resonators and band-pass filters.[1–3] Such films have been prepared by metalorganic chemical vapor deposition (MOCVD), pulsed laser deposition (PLD), and magnetron sputter deposition.[4–6] In most cases, highly *c*-axis oriented films are crucially important for optimizing both the electromechanical coupling coefficient K_t^2 and the Q value of electro-acoustic devices, since they can excite pure longitudinal mode along the thickness direction.[7,8] However, operating in liquid media, shear-mode resonance instead of longitudinal-mode resonance is required for biochemical sensors, because the longitudinal wave produces compressional motion and leaks acoustic energy into the liquid media, resulting in reduced resolution.[9] Therefore, AlN and ZnO films with tilted textures are desired, since they can potentially excite dual-mode resonance (both longitudinal and shear modes), which is beneficial for biochemical sensing applications. Indeed, the transverse polarization of shear modes is more sensitive than the vertical polarization of longitudinal modes, because the former does not produce any compressional motion in the liquid media. Hence, no energy leakage occurs and sensors achieve better resolution.[10,11] Therefore, *c*-axis tilted AlN films rather than perfectly *c*-axis oriented films are desired to improve the shear electromechanical coupling coefficient in biochemical sensors.

To optimize the shear electromechanical coupling coefficient, the *c*-axis inclination angle should be in the range of 5° to 30°.[12] Several methods have been developed in the past decade to deposit tilted AlN and ZnO thin films. Hunt and coworkers developed a method using an additional electric field during the sputter deposition to promote *c*-axis inclination of ZnO films.[13] Yanagitani et al. first produced *c*-axis tilted AlN films in a planar deposition system.[14] Later, Elmazria and coworkers used a tilted substrate to grow tilted ZnO films.[15] Recently, Link et al. applied an additional blind positioned between

(Received November 2, 2010; accepted April 26, 2011; published online May 17, 2011)

the target and the substrate to fabricate *c*-axis tilted ZnO films.[16]

In this study, AlN films were deposited on Pt-coated silicon substrates in an off-center system without additional hardware modification or substrate tilting. The microstructure and morphology of as-deposited films were characterized by means of scanning and transmission electron microscopy and x-ray diffraction. Highly dual-mode solidly mounted resonators (SMRs) based on the deposited AlN films were fabricated to investigate the excitation of shear modes and assess the piezoelectric properties of the films. The dual-mode SMRs are aimed at applications in bio- and viscosity sensors.

EXPERIMENTAL PROCEDURES

AlN thin films were reactively deposited on a *p*-type (100) silicon wafer coated with a 100 nm Pt layer in a radio frequency (RF) magnetron sputtering system (JGP 450). The target was a 99.995% pure Al disk, 60 mm in diameter, and nitrogen/argon gas mixture was employed. The system was pumped down to a base pressure of less than 2×10^{-4} Pa. The substrate temperature was kept at 300°C, the nitrogen concentration in the N_2/Ar gas mixture was 60%, and the pressure was fixed at 0.5 Pa. A RF power of 200 W was applied to the cathode for 1 h. The target–substrate distance was 5 cm.

In the present study, deposition of AlN films was again accomplished by a conventional magnetron sputtering method, except that the substrate was mounted off center with respect to the target. As a result, rotation of the substrate holder plate (as shown in Fig. 1) is expected to change the angle of deposition. During the deposition, the rotation angle of the substrate was allowed to assume the values 0°, 5°, 10°, and 15°. Preparation at a rotation angle of 0° means that the substrate is located at the center of the target.

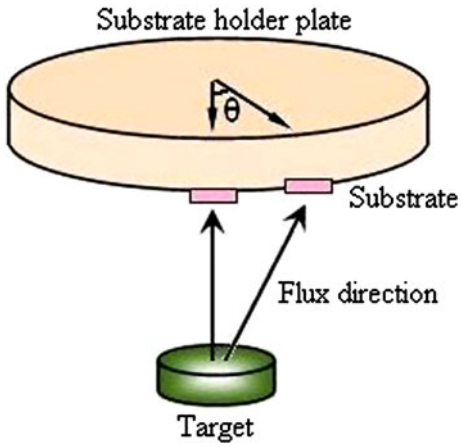

Fig. 1. Schematic configuration of AlN deposition by rotating the substrate holder plate to different angles.

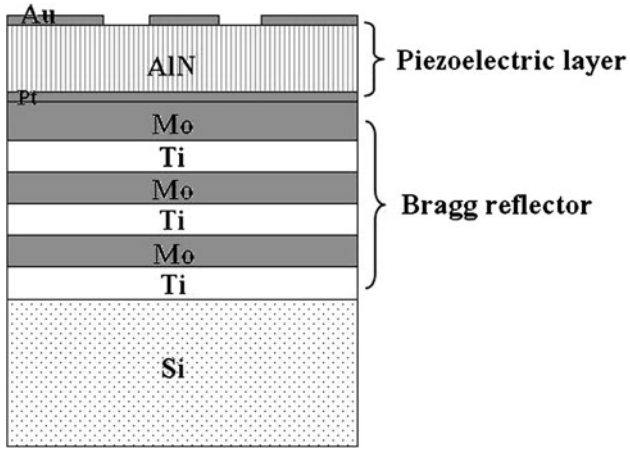

Fig. 2. Schematic structure of the SMR device.

X-ray diffraction (XRD, D8; Bruker) with Cu K_α (λ = 0.15406 nm) radiation was used to determine the crystalline properties of the AlN thin films in terms of preferred orientation and *c*-axis inclination. The morphology of the films was observed by field-emission scanning electron microscopy (FESEM, S-4800; Hitachi). Transmission electron microscopy (TEM, JEM-2010F; JEOL) operating at 200 kV and selected-area electron diffraction (SAED) were used to investigate the microstructure as well as the *c*-axis inclination of AlN films. Cross-sectional TEM samples were prepared at room temperature following standard procedures of face-to-face gluing, mechanical thinning, dimpling, and ion milling with a 5-keV beam and beam-to-specimen surface angle of 3° to 5°.

Finally, to investigate the shear mode generation in the deposited films, a dual-mode SMR was fabricated to assess the piezoelectric activity of the AlN films. The dual-mode SMR was composed of a *c*-axis inclined AlN film sandwiched between a 100 nm Pt bottom electrode and a 100 nm Au top electrode, and Mo/Ti high/low acoustic impedance layers, all obeying the $1/4\lambda$ mode resonance criteria, and a *p*-type (100) Si substrate, as shown in Fig. 2. RF/direct-current (DC) magnetron sputtering and photolithography were used to fabricate the required multilayer structure. The bottom electrode served as the electrical ground plane, and the top electrode was patterned in ground–signal–ground configuration for measurements using an Agilent 4291B network analyzer and a Cascade probe station, in which the standard RF on-wafer measurement technique was employed. The active device area was 100 μm × 100 μm. When an electrical signal was applied between the top and bottom electrodes, an acoustic wave was excited in the AlN film.

RESULTS AND DISCUSSION

The *c*-axis inclined AlN films were deposited on a 100 nm Pt bottom electrode layer with the substrate holder plate rotated to different angles. θ–2θ x-ray

scans showed a (002) *c*-axis preferred orientation for all AlN films except for the one deposited at a rotation angle of 15°, which exhibited an additional (100) diffraction, as shown in Fig. 3. However, a significant decrease in (002) peak intensity was clearly observed as the rotation angle increased. This results from the decreased energy of plasma species due to a decrease in the mean free path at large rotation angle. Consequently, particles with decreased energy bombard the surface of the layer, leading to decreased adatom mobility and thus the decreasing (002) peak intensity or the appearance of (100) and (101) peaks.

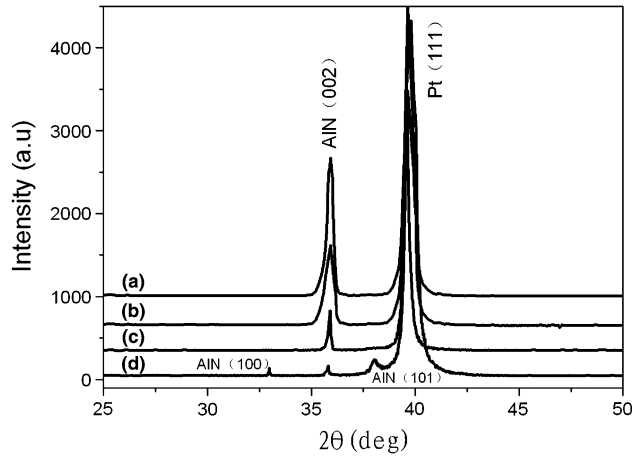

Fig. 3. XRD patterns of AlN films deposited by rotating the substrate holder plate to an angle of (a) 0°, (b) 5°, (c) 10°, and (d) 15°.

Morphological characterization of AlN films deposited at different rotation angles was performed by FESEM analysis, as shown in Fig. 4. AlN columns inclined from the surface normal were clearly observed. The column inclination estimated from FESEM images varied from 5° for the sample deposited at a rotation angle of 5°, to 12° for the sample deposited at a rotation angle of 10°. The larger the rotation angle of the substrate holder plate, the more inclined the crystalline orientation obtained. In fact, for a rotation angle of 0°, the grains of the deposited film remained vertical, while the columnar structure disappeared in the AlN film deposited at a rotation angle of 15°, consistent with the XRD results. From these analyses, it can be deduced that the film exhibits *c*-axis inclined columnar structure with oblique incidence flux and sufficient energy, and the *c*-axis inclination disappears as the flux direction deviates further from the center of the substrate.

Figure 5a presents a TEM bright-field image for the sample deposited by rotating the substrate holder plate to an angle of 5°. The cross-sectional

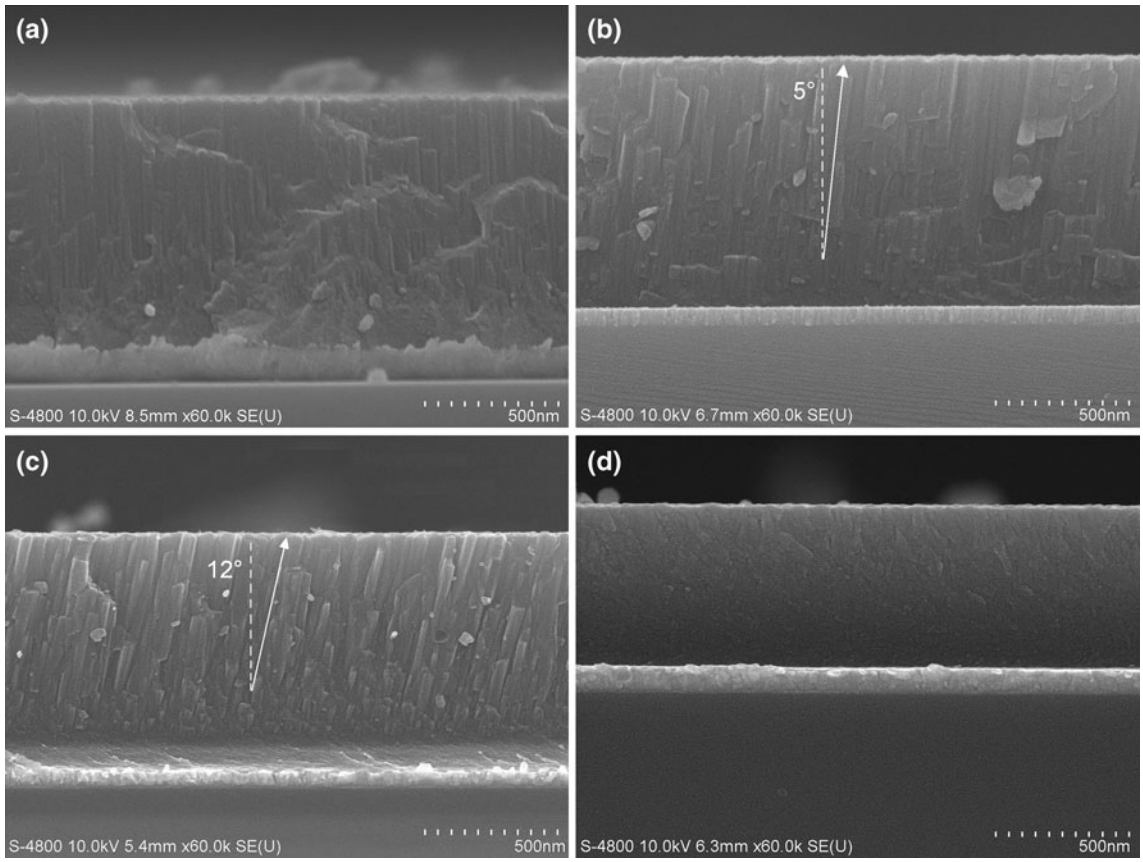

Fig. 4. Cross-sectional FESEM images of AlN films deposited by rotating the substrate holder plate to an angle of (a) 0°, (b) 5°, (c) 10°, and (d) 15°.

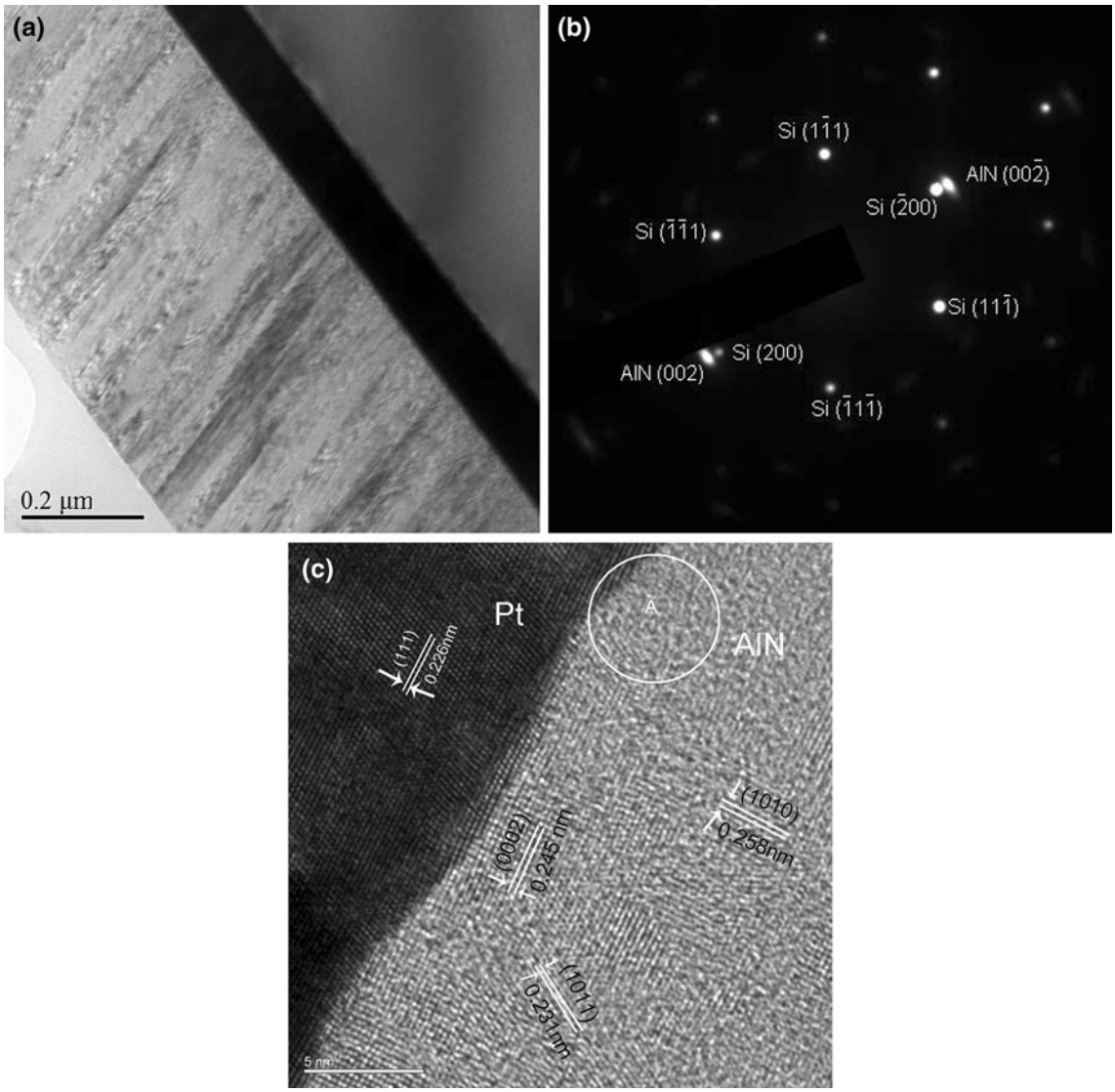

Fig. 5. (a) TEM cross-section bright-field image of *c*-axis inclined AlN films on the Pt bottom electrode, (b) SAED pattern, and (c) high-resolution TEM image of the cross-section at the interface between Pt and AlN layers.

TEM image shows the columnar structure of the film and *c*-axis inclined orientation of about 5°, which is well consistent with the FESEM result shown in Fig. 4. On the other hand, there is no evidence of a secondary-phase interfacial layer between the Pt and AlN films. The TEM image reveals that the AlN film is uniform and dense, and the interfacial region shows a smooth and sharp interface. It is worth noting that the roughness of the layers is critical for the acoustic wave scattering loss, since a rough surface or interface leads to energy scattering and induces dissipation loss in microwave applications.[17] In the SAED pattern (Fig. 5b), the electron beam was parallel to the [100] direction of the silicon substrate, and the diffraction was taken from an area in close proximity to the film interface. The well-defined electron diffraction spots without the ring pattern characteristic of polycrystalline grains indicate excellent film crystallinity.

Figure 5c shows a high-resolution TEM image of the cross-section around the interface between the Pt and AlN films. There is an inhomogeneous transition layer, approximately 5 nm thick, in the area marked A. The reason for the appearance of this transition layer is partly due to the decreasing adatom mobility with oblique incidence. It is also likely due to lattice mismatch between the AlN film and the Pt bottom electrode layer. (002), (100), and (101) orientations of AlN are observed around the interface between the Pt and AlN layers. There is only (002) preferred orientation in the area approximately 20 nm away from the interface (data not shown).

Many investigations have addressed the growth mechanism of inclined AlN films. Lobl et al. pro-

posed that, in the case of the following direction of the impinging source material with a small angle, the (002) plane was almost always perpendicular to the normal of the surface, and the column inclination was due to the shadowing effect.[18] Martin suggested a second growth mechanism, according to which the (002) planes always grew in a direction perpendicular to the substrate in order to minimize the surface energy and the inclined columns were a result of the oblique incidence.[19] In our case, the grains are quasivertical (inclination of 0° to 2°) to the film surface at a low pressure of 0.5 Pa. The transformation from quasivertical to tilted growth (*c*-axis inclination of up to 5°) could be induced by decreased adatom mobility due to the oblique flux at low pressure as well as by the shadowing effect. The low adatom mobility prevents adatoms from jumping at the surface and induces atomic rearrangement resulting in a *c*-axis perpendicular to the surface. Actually, oblique incidence is due to the cosine distribution of the sputtered particles, which also explains the fact that no *c*-axis inclination was obtained in the sample deposited at a rotation angle of 0°. So, atoms arriving at the substrate with oblique incidence are more apt to induce tilted columns.

However, it has often been observed that the buffer layer or substrate orientation plays a key role in the growth of a tilted AlN thin film.[20,21] Meanwhile, the film also needs some islands exhibiting preferred orientation in the direction of the sputtering flux in the nucleation phase in the case of AlN deposited on a Pt-coated substrate. Therefore, a substrate which facilitates nucleation of inclined islands, or that creates conditions for inclined islands and grain growth, is favorable. In our case, the lattice mismatch between the AlN (002) plane and the Pt (111) plane is only 6.9% with nanoscale surface roughness, which leads to a large number of inclined islands,[22] meaning that columns that are aligned with the inclined net flux direction grow faster than columns in other directions due to competitive growth. The induction of *c*-axis inclination is facilitated by the Pt film. Impinging particles are deposited on the tilted surface due to the nanoscale surface roughness and the small lattice mismatch between the AlN film and the Pt layer.

To clarify the generation of shear mode waves in the obtained AlN films, SMR devices based on the vertical and *c*-axis inclined (by 12°) AlN films were fabricated. The resulting frequency responses, S_{11}, are shown in Fig. 6, illustrating distinct resonance behavior and excellent noise restraint. Moreover, dual-mode resonance is clearly observed with the fundamental longitudinal and thickness shear modes located at 1.87 GHz and 1.12 GHz, respectively. Considering the wavelength value, the shear velocity was calculated to be 6510 m/s, which is close to the shear mode velocity in AlN films (6330 m/s).

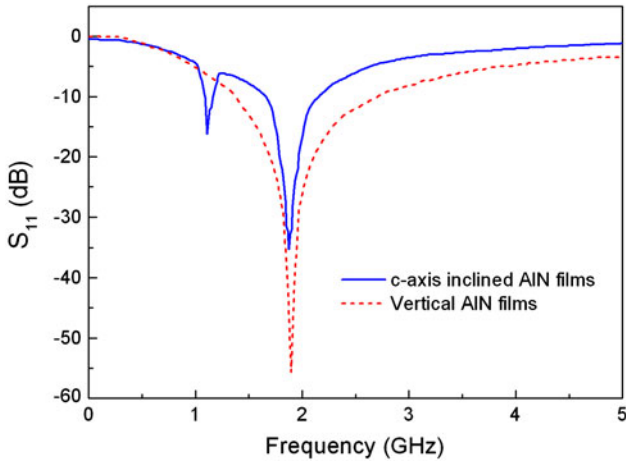

Fig. 6. Frequency responses, S_{11}, of SMRs with vertical and *c*-axis inclined (by 12°) AlN films.

However, the longitudinal resonance is suppressed for the *c*-axis inclined AlN SMR, as shown in Fig. 6. The suppression effect results from two main factors. Firstly, in the off-center deposition process the density of the AlN film was decreased, thus the degree of *c*-axis orientation was degraded, as evidenced by the weak peak in the XRD pattern. Secondly, since the AlN crystallites are tilted, the acoustic wave attenuation increases, resulting in suppression of the longitudinal resonance. The frequency response characteristics present an insertion loss of −34.8 dB and a rejection loss of −3.9 dB. The performance of the dual-mode SMR could be improved by increasing the *c*-axis inclination or by optimizing the SMR design. Further work on processing optimization to improve the performance of such devices for biochemical sensing applications is in progress.

CONCLUSIONS

Highly *c*-axis inclined AlN thin films were prepared on Pt-coated Si substrates. By rotating the substrate holder plate in the magnetron sputtering system without additional hardware modification or substrate tilting, *c*-axis inclination of up to 12° could be produced for the given deposition conditions. The oblique incidence of the particle flux and the small lattice mismatch between the AlN (002) plane and the Pt (111) plane with nanoscale roughness are responsible for the formation of *c*-axis inclined films. The inclined AlN films were tested by fabricating SMR devices, and the frequency responses showed resonant characteristics at 1.12 GHz and 1.87 GHz, corresponding to shear and longitudinal mode resonances, respectively. The results show that *c*-axis inclined AlN films are promising candidates for biochemical sensing applications.

ACKNOWLEDGEMENTS

This work was funded by the National Natural Science Foundation of China (NSFC) (Grant No.

61076049), the Science Foundation of Scientific Bureau of Guangdong Province (Grant No. 2009B 090300368), and the International Collaboration Program of Wuhan (Grant No. 201070934340).

REFERENCES

1. A.F. Mammeri, M.B. Assouar, and O. Elmazria, *Semicond. Sci. Technol.* 23, 095013 (2008).
2. G. Sharma, L. Liljeholm, J. Enlund, and J. Bjurström, *Sens. Actuators A* 156, 111 (2010).
3. X.Y. Du, Y.Q. Fu, J.K. Luo, and A.J. Flewitt, *J. Appl. Phys.* 105, 024508 (2009).
4. L. Mai, V.S. Pham, and G. Yoon, *Appl. Phys. A* 95, 667 (2009).
5. M. Imura, K. Nakajima, M. Liao, and Y. Koide, *J. Cryst. Growth* 312, 1325 (2010).
6. A. Artieda, M. Barbieri, C.S. Sandu, and P. Muralt, *J. Appl. Phys.* 105, 024504 (2009).
7. H. Campanella, A. Uranga, J. Montserrat, and G. Abadal, *Sens. Actuators A* 142, 322 (2008).
8. R.C. Lin, Y.C. Chen, W.T. Chang, and C.C. Cheng, *Sens. Actuators A* 147, 425 (2008).
9. C.J. Chung, Y.C. Chen, and C.C. Cheng, *Sens. Actuators A* 156, 180 (2009).
10. G. Wingqvist, H. Anderson, C. Lennartsson, T. Weissbach, V. Yantchev, and A.L. Spetz, *IEEE Trans. Ultrason., Ferroelect., Freq. Contr.* 55, 857 (2008).
11. E. Milyutin, S. Gentil, and P. Muralt, *J. Appl. Phys.* 104, 084508 (2008).
12. F. Martin, M.E. Jan, and B. Belgacem, *Thin Solid Films* 514, 341 (2006).
13. C.D. Corso, A. Dickherber, and W.D. Hunt, *J. Appl. Phys.* 101, 054014 (2007).
14. T. Yanagitani, M. Kiuchi, M. Matsukawa, and Y. Watanabe, *J. Appl. Phys.* 102, 024110 (2007).
15. S. Benmaine, L.L. Brizoual, O. Elmazria, and J.J. Fundenberger, *Phys. Stat. Sol. (a)* 204, 3091 (2007).
16. M. Link, M. Schreiter, J. Weber, and R. Gabl, *J. Vac. Sci. Technol.* 24, 218 (2006).
17. B. Ivira, P. Benech, R. Fillit, and F. Ndagijimana, *IEEE Trans. Ultrason. Ferroelect. Freq. Contr.* 55, 421 (2008).
18. H.P. Lobl, M. Klee, R. Milsom, and R. Dekker, *J. Eur. Ceram. Soc.* 21, 2633 (2001).
19. F. Martin, M.E. Jan, S.R. Mermet, and B. Belgacem, *IEEE Trans. Ultrason. Ferroelect. Freq. Contr.* 53, 1339 (2006).
20. M. Clement, J. Olivares, E. Iborra, N. Rimmer, and A. Rastogi, *Thin Solid Films* 517, 4673 (2009).
21. T. Riekkinen, A. Nurmela, J. Molarius, and T. Pensala, *Thin Solid Films* 517, 6588 (2009).
22. J.B. Lee, J.P. Jung, M.H. Lee, and J.S. Park, *Thin Solid Films* 447–448, 610 (2004).